MEASUREMENTS OF ATMOSPHERIC WATER PARAMETERS AND WIND SPEED WITH THE SPECIAL SENSOR MICROWAVE/IMAGER AND THE ERS-1 SCATTEROMETER

Kristina B. Katsaros
Department of Atmospheric Sciences AK-40
University of Washington
Seattle, WA 98195 - USA

and

Departement d'Océanographie Spatiale
Institut Francais de Recherche pour L'Exploitation de la Mer
Centre de Brest, B.P. 70
29280 Plouzané - France

Summary: The Special Sensor Microwave/Imagers on satellites in the U.S. Defense Meteorological Satellite Program provide data on integrated atmospheric water vapor, cloud liquid water, and precipitation over the ocean. In addition, near surface wind speed can be retrieved when the emission, absorption, or scattering by the various forms of atmospheric water listed above is low.

The instrument characteristics and the principles of data interpretation are presented. Application to studies of storms, verification of cloud models, and climate models are discussed. Synergetic use of the SSM/I atmospheric water parameters with other satellite data; in particular, the vector-wind fields from the scatterometer on the European Remote Sensing Satellite-1 (ERS-1) are suggested for new insights into the structure of cyclones of all types from typhoons and hurricanes to midlatitude frontal systems and polar lows.

1. INTRODUCTION

Microwave radiometry from space has been employed for more than two decades to study atmospheric properties, sea ice and earth surface properties such as soil moisture content and vegetation or snow cover (e.g., Lipes *et al.*, 1979; Njoku and Swanson, 1983; Gloersen *et al.*, 1984; Katsaros and Brown, 1990). This review will be dedicated to the current passive microwave radiometer in space, the Special Sensor Microwave/Imager (SSM/I), operating since 1987 on several satellites in the U.S. Defense Meteorological Satellite Program (DMSP). Data are available in near real time at several meteorological and sea ice forecast centers and are freely available for research purposes through the NASA WETNET program*. This review is limited to meteorological or sea surface studies employing SSM/I, and extends the report by Katsaros (1988) written for a previous ECMWF seminar.

Microwave radiometry allows measurement of the atmospheric water content over the sea. Integrated water vapor, cloud liquid water, and qualitative estimates of precipitation intensity can be retrieved from SSM/I brightness temperatures. At the microwave frequencies of SSM/I the high level cirrus clouds are completely transparent, in contrast to their appearance at infrared wavelengths where the penetration depth is of the order of 20m.

The lack of measurements of cloud liquid water and precipitation over the sea gives the microwave radiometer data their unique value. Coastal radars provide similar information and can be used to advantage in calibration of the microwave precipitation algorithms (e.g., Petty and Katsaros, 1992a) but over the open ocean, SSM/I currently provides the most direct measurements. Other indirect methods for estimating precipitation over the sea using visible and infrared satellite data have a much longer history and the geostationary satellites providing the data have better temporal sampling (e.g., Griffith *et al.*, 1978; Adler and Negri, 1988 and references therein).

Physical principles, instrument characteristics, and algorithms, are presented followed by examples of applications. In the final section use of SSM/I information with surface wind observations by the scatterometer on the European Remote Sensing Satellite-1 (ERS-1) are discussed.

---

* Contact person: Dr. James Dodge, Manager, Mesoscale Processes Research Program, Code EBT8, NASA Headquarters, Washington, D.C. 20546.

2. BACKGROUND

2.1 Physical principles

Being that microwave radiometers are passive instruments, they respond to emitted, reflected, and scattered signals from the ocean and the atmosphere. The atmosphere is relatively transparent at microwave frequencies. The interpretation depends on the microwave frequency being used and the complexity of the scene viewed by the satellite. These two facts contribute to a certain ambiguity in interpreting microwave radiometer data. A comprehensive introduction to the interpretation of atmospheric and sea surface signals in the SSM/I frequency range is provided by Petty (1990; 1994), and Petty and Katsaros (1992b, 1994). For microwave radiation, the Planck function for thermal emission can be simplified to the Rayleigh-Jeans approximation; radiance is simply proportional to the thermodynamic temperature of the radiating medium. This has given rise to use of the term "brightness temperature", T_B, for radiance which has units of degrees Kelvin:

$$T_B = L = \frac{\partial B(\lambda,T)}{\partial \varpi} \tag{1}$$

where: B is black body radiance, w is solid angle, L is radiance, T is temperature, and T_B is brightness temperature, equivalent to radiance.

The ocean surface emits microwave radiation of feeble intensity, because its emissivity is only of the order of 0.5. Thus, the T_B of the sea is about 150K for a surface temperature of 300K. The microwave radiometers in use during the last decades operate in both horizontal and vertical polarization and the emission from the sea is strongly polarized, T_{BV} - T_{BH} being of the order of 20K (where subscripts V and H refer to vertical and horizontal polarization; e.g., Petty and Katsaros, 1994). Petty (1990) and Petty and Katsaros (1994) employ the most recent electromagnetic constants for water and use Fresnel theory to calculate the polarized emittance at the SSM/I frequencies. The emissivity and the polarization are dependent on the roughness of the sea and therefore on the near surface wind speed (Nordberg *et al.*, 1971; Wentz, 1983; Petty and Katsaros, 1994).

Emission from water vapor and oxygen are responsible for the signals from the clear atmosphere (Figure 1). The weak absorption band at 22 GHz is used to measure the integrated atmospheric water vapor above the sea. Because this water vapor band is weak, even in the moist tropical atmosphere this band does not become opaque and the evaluation of water vapor content remains good (e.g., Katsaros, 1988; Alishouse *et al.*, 1983). However, thick precipitating clouds saturate the signals and make estimates of integrated water vapor erroneous.

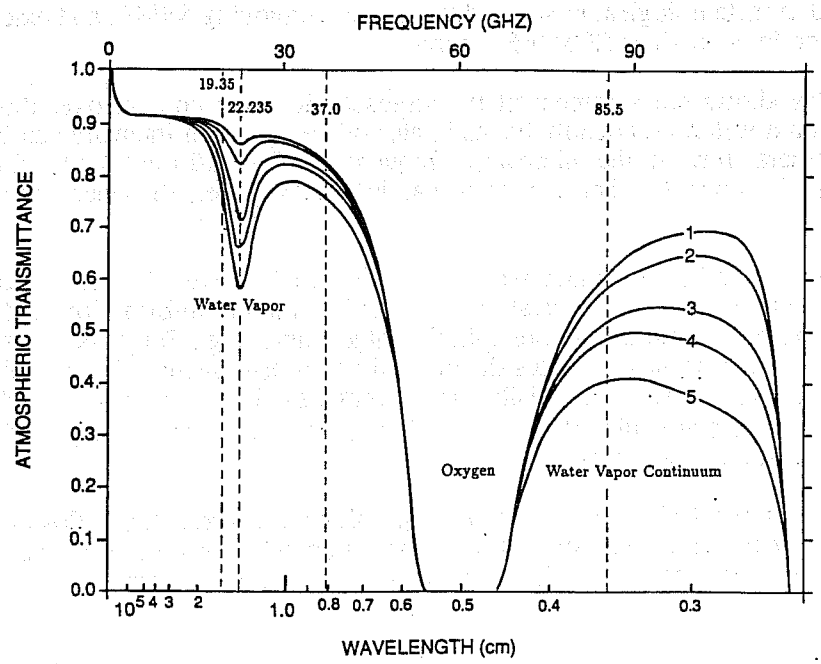

Fig. 1 Total atmospheric microwave transmission for a zenith angle of 53°. Model atmospheres used are (1) wintertime polar, (2) summertime polar, (3) wintertime midlatitude, (4) summertime midlatitude, and (5) tropical. Plots were generated using the FASCOD3 line-by-line code package (Clough et all 1989,after Petty 1990).

At 85 GHz the signals are sensitive to another water vapor band. This higher frequency is mostly employed to detect scattering by large cloud ice particles or to estimate integrated cloud liquid water (ICLW) in stratus clouds (e.g., Petty and Katsaros, 1990a; Miletta, 1993). A correction for the water vapor content should be made when using this frequency.

The attenuation of the sea surface emission by the atmosphere allows interpretation of the absorption and/or scattering properties of the intervening clouds. Petty (1990) develops the radiative transfer equation of the brightness temperature observed by a satellite instrument in terms of the polarized emissivity ε_p, and the depolarized diffuse reflection by the sea surface. Thus:

$$T_B(\mu,\phi) = T_B^{\uparrow}(\mu) + \tau(0,\infty)\left[\varepsilon_p(\mu,\phi)T_S + \frac{1}{\pi}\int_0^{2\pi}\int_0^1 r_p(\mu,\phi;\mu',\phi')\mu' T_B^{\downarrow}(u')d\mu'\,d\phi'\right] \quad (2)$$

where: μ and μ' are the cosine of vertical incidence and reflection angles θ and θ'
ϕ and ϕ' represent azimuth angles of incidence and scatter
$T_B^{\uparrow}$ and $T_B^{\downarrow}$ represent the upward radiance at the top of the atmosphere and the downward radiance at the sea surface, respectively
$\tau(\mu,\phi)$ is the transmittance by the whole atmospheric column in the direction (μ,ϕ)

Subscripts for microwave wavelength have been suppressed; however, all these parameters are wavelength dependent. (See further Petty, 1990, Chapter 5; Sand, 1992; and Adler *et al.*, 1989 for details.)

The schematic in Figure 2 illustrates the SSM/I sensitivities to atmospheric phenomena.

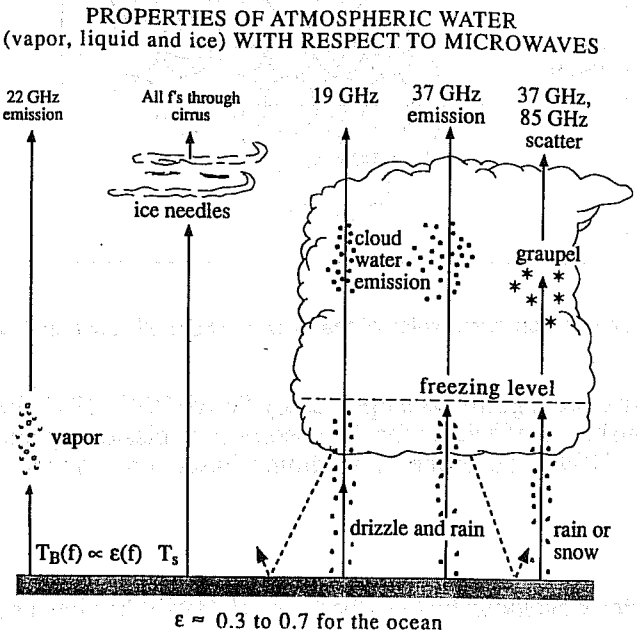

Fig. 2 Schematic of atmospheric transmission and scattering emission at SSM/I frequencies. (After Katsaros, 1992)

2.2 The Special Sensor Microwave/Imager

The SSM/I is described by Hollinger *et al.* (1987). It is launched on satellites in the operational F-series of the Defense Meteorological Satellite Program (DMSP). Satellites F8, F10 and F11 have been equipped with SSM/Is; the last two are still operating at the end of 1993. Table 1 lists frequencies and surface resolution of this instrument. The DMSP satellites are in sun-synchronous orbit at about 860 km elevation with a 98.8 inclination. Their equatorial crossing times are near dusk and dawn. A conical electrical scan sweeps out a 1400 km swath aft of the satellite with samples organized as seen in Figure 3.

2.3 Algorithms for meteorological parameters

Several algorithms have been developed for use with SSM/I. The prelaunch algorithms, (the so-called D-matrix) were discarded almost immediately. Several operating versions of algorithms exist (e.g., Wentz, 1983; Alishouse *et al.*, 1990a,b; Petty and Katsaros, 1990; Petty, 1994) and some future refinements are

TABLE 1: The frequencies, wavelengths and resolutions of the Special Sensor Microwave/Imager. Effective 3-dB spatial resolution for SSM/I channels.

Frequency	*Polarization*	*Wavelength*	*Along-Track*	*Along-Scan*
19.35 GHz	H, V	15.5 mm	69 km	43 km
22.235 GHz	V	13.5 mm	50 km	40 km
37.0 GHz	H, V	8.1 mm	37 km	29 km
85.5 GHz	H, V	3.5 mm	15 km	13 km

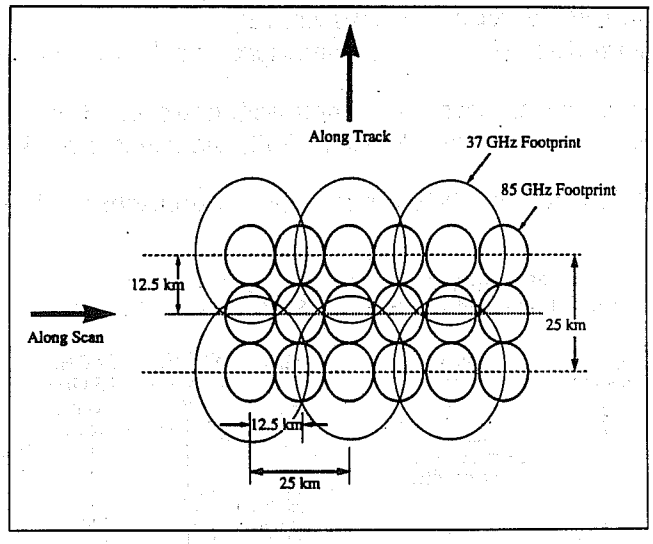

Fig. 3 Spatial and sampling characteristics of the 37.0 and 85.5 GHz channels (after Miletta 1993).

still likely. Here I emphasize the algorithms employed by Petty (1990, 1994) because they have been used in my group. Using established coefficients for the absorption/emission by atmospheric gases and for sea surface emissivities Petty (1990) developed algorithms based on empirical fits to radiative transfer calculations.

Surface wind speed

For wind speed the expression developed by Goodberlet *et al.* (1989) has been generally adopted:

$$U(ms^{-1}) = 1.0969T_{19V} - .4555T_{22V} - 1.760T_{37V} + .7860T_{37H} + 147.90 \quad (3)$$

A rain flag must be applied to avoid using rain contaminated pixels. In rain-free areas, the SSM/I wind estimates have been found to be within 2 m/s of buoy measurements (Goodberlet *et al.*, 1989) and other estimates obtained from active microwave instruments in space, such as the Geosat altimeter (Mognard and Katsaros, 1994a) or the ERS-1 scatterometer (A. Bentamy, personal communication). Figure 4 shows the SSM/I and Geosat wind speed comparison cited above, i.e., with low atmospheric liquid water content in the column and temporal separation of the observations < 1 hr.

Water vapor

For water vapor a regression between a large radiosonde data set and measured SSM/I radiances resulted in an expression for integrated water vapor IWV in close agreement with the expression given by Alishouse *et al.* (1990a). Petty's formula is:

$$V(kg\ m^{-2}) = 174.1 + 4.638\log(300 - T_{19H}) - 0.6176\log(300 - T_{22H}) + 19.58\log(300 - T_{37H}) \quad (4)$$

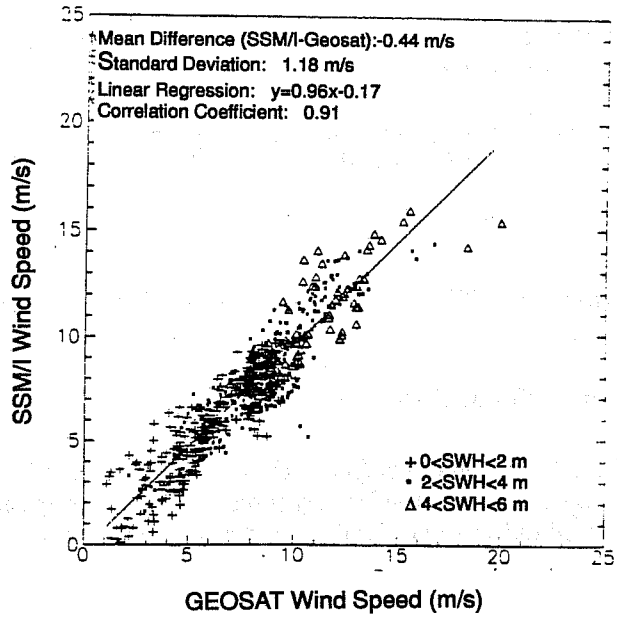

Fig. 4 Comparison of wind speed measurements by the Geosat altimeter and the SSM/I radiometer with time difference < 1h for low cloud liquid water content. (After Mognard and Katsaros, 1994a)

Integrated cloud liquid water

For cloud liquid water we use the 37.0 and 85.5 GHz channels. The algorithms are based on a parameter called the normalized polarization difference, P, which is the observed polarization difference at a given frequency normalized by an estimate of the polarization difference in the absence of clouds under otherwise similar meteorological conditions. P_{85} and P_{37} are given by eqs. (5) and (6):

$$P_{85} = (T_{85V} - T_{85H})\exp(.0241U + .0271V - 4.44) \tag{5}$$

$$P_{37} = (T_{37V} - T_{37H})\exp(.0151U + .00607V - 4.40) \tag{6}$$

In case of stratus decks with no overlying ice containing clouds, Petty's (1990) calculation indicate the following expressions for cloud liquid water:

$$L_{85}(kg\,m^{-2}) = -0.339\log_e(P_{85}) \tag{7}$$

$$L_{37}(kg\,m^{-2}) = -1.42\log_e(P_{37}) \tag{8}$$

"Advantages of L_{37} over L_{85} include reduced sensitivity to the effects of variations in water vapor and to precipitation size particles, as well as greater linearity in the response of 37 GHz channels to liquid water (hence reduced errors due to inhomogeneity within the satellite footprint). Disadvantages include significantly poorer spatial resolution (30 km vs. 15 km) and, in middle and high latitudes (i.e., for low water vapor amounts), somewhat poorer signal-to-noise ratio" (Petty, 1990). Young *et al.* (1992) showed that these algorithms were consistent with measurements from a surface based radiometer.

Precipitation

After experience with SMMR rain algorithms and comparisons to radar estimates (Petty and Katsaros, 1990b) we provide a precipitation index whose values are proportional to rain water in the column. A single general rain rate algorithm is not likely to be found for the global oceans. However, for similar types of precipitation systems a relationship can usually be defined through empirical fits. Large hydrometers influence the upwelling microwave radiation by absorption of the ocean signals and emissions from the drops themselves. They also cause scattering. The effects depend on the ratio of electromagnetic wavelength to the diameter of the droplet cross-section. Both emission and scattering based algorithms have been proposed (e.g., Wilheit and Chang, 1980; Spencer, 1986; Petty 1990; 1994b).

The normalized polarization index, P_{37} measures the depolarization of the sea surface signals by the cloud mass including precipitation particles. The expression for P_{37} (eq. 6, above) is used to indicate precipitation when $P_{37}<0.8$ (Petty and Katsaros, 1990a).

Scattering by the precipitation size ice particles is quantified by a scattering index based on either the 37 or 85.5 GHz channels (e.g., Spencer, 1986; Petty and Katsaros, 1990). For 85 GHz it is defined by:

$$S_{85}(K) = P_{85}T_{85V,O} + (1 - P_{85})T_C - T_{85V} \tag{9}$$

T_C is an assumed cloud temperature, 273K. $T_{85V,O}$ is the brightness temperature for the nearby cloud free ocean, and is calculated by:

$$T_{85V,O} = 280.0 - \exp(4.20 - .00567U - .0406V) \tag{10}$$

where U and V are determined from equations (3) and (4). Corrections for atmospheric water vapor, V, and effects of surface wind speed, U, on the background emission are taken into account by the term $T_{85V,O}$. No direct empirical calibration exists for these indices in terms of precipitation.

3. APPLICATIONS

This review of applications of SSM/I measurements to meteorology does not attempt to be exhaustive, but will highlight a few examples.

Detection of mesoscale cloud and precipitation features

Rain cells identified by SMMR off the Oregon and Washington coasts were tracked and identified in coastal rain gauge data (Katsaros and Lewis, 1986). McMurdie *et al.* (1987) discuss frontal waves and convergence zones using Seasat SMMR and scatterometer information. Miletta (1993) discusses the rain patterns along the fronts of a midlatitude cyclone and their relation to the overlying clouds seen in infrared by the Optical Linescan System also on the DMSP satellites. The scattering ice index revealed the presence of a polar low, when numerical model and operational satellite data were not detecting it (Claud *et al.*, 1992). Claud *et al.* (1993) have extended this work and evaluate multi-satellite observations of polar lows, which could give early warning of their existence, and provide new information about their genesis and structure. Curry *et al.* (1990) used observations by SSM/I to infer cloud liquid water and precipitation characteristics of stratus clouds.

Midlatitude cyclones

Previous work employing SMMR to study midlatitude cyclones (e.g., McMurdie and Katsaros, 1985; McMurdie and Katsaros, 1991; Katsaros *et al.*, 1989) can be applied equally well to SSM/I (Miletta, 1993; Mognard and Katsaros, 1994b). Figure 5 is a schematic of the relationship of the integrated water vapor signal from SSM/I to frontal locations at various stages of cyclone development. An index of the magnitude of the water vapor gradient was used to locate fronts in the study by Katsaros *et al.* (1989). It was dependable about 90% of the time using SMMR data and was tried successfully for the SSM/I, but without a statistical test. Exact location of the surface front with respect to the cloud features seen in visible or infrared images, or to the patterns in the SSM/I parameters is currently under debate. For example, a well documented case (Reed *et al.*, 1993) shows the upper cloud features ahead of the surface front. In the same study, the rain areas in the NCAR mesoscale model simulation of the rapidly deepening cyclone compared well to SSM/I estimates.

Tropical storms

SSM/I averages around tropical storm centers were used by Glass and Felde (1992) to develop a relationship with storm intensity defined in terms of maximum surface wind speed $\overline{U}_{MAX}$ near the center. Similar tests were done on a larger data set by Katsaros *et al.* (1993) and were in general agreement that a close relationship existed between maximum surface wind and the distribution of convective rain cells. Quilfen *et al.* (1994) combined ERS-1 scatterometer derived surface wind analysis with SSM/I fields to illustrate this correlation but without quantitative evaluation (Figure 6), since current ERS-1 algorithms are not calibrated beyond 25 m/sec. Effects of the limited (50 km) resolution and interference by clouds and rain, and effects of rain impact on the sea surface and of the extreme sea states developing in such storms are discussed briefly by Quilfen *et al.* (1994). Further work on extreme events employing ERS-1 and

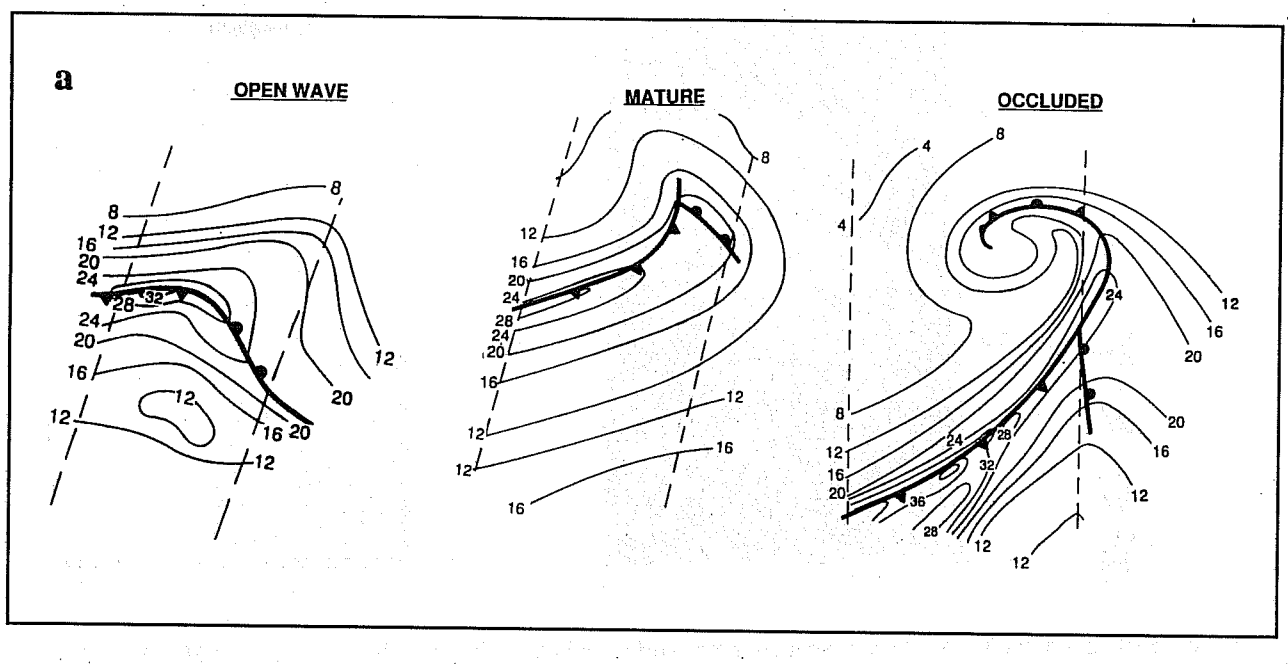

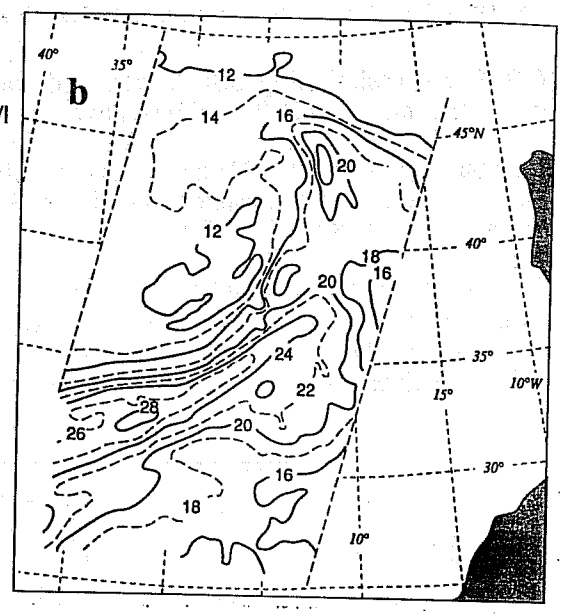

Fig. 5 Examples of integrated water vapor patterns in mid-latitudes.
a) Schematic at three stages,
b) example from the occluded stage orbit 3103 of the SSM/I on F8.

SSM/I data should be profitable both for advancing the knowledge about the storms and for better understanding of the functioning of the microwave sensors.

Forecasting

The Seasat scatterometer was successfully used to identify surface fronts by Peteherych *et al.* (1988) and improved short range forecasts for the coastal region off British Columbia. Snapshots of the water vapor distribution from SSM/I in the Gulf of Mexico were shown to indicate the region of northward progressing moist air over the United States (Rabin *et al.*, 1991). The location of this moist air mass is important for forecasting thunderstorm outbreaks. It appears that real-time SSM/I observations of precipitating systems at mid-latitudes, polar regions, and in tropical regions represent good use of the mesoscale information in these satellite data. Similarly, the ERS-1 wind vectors in swath format at 50 km resolution received in near-real time provide valuable warning of unusual and unpredicted wind features.

Model verification and assimilation

Use of microwave data from SMMR and SSM/I have been slow to be used with numerical models in part due to the difficulties of assimilating asynoptic swath-confined data. However, early comparisons between the most dependable microwave parameter, the integrated water vapor, suggested an overabundance of water vapor in the model of the European Center for Medium Range Weather Forecasts (ECMWF) (Katsaros *et al.*, 1990; McMurdie and Katsaros, 1991). Liu *et al.* (1992) similarly compare SSM/I and ECMWF data for the distribution of integrated water vapor and surface humidity. Robertson and Cohen

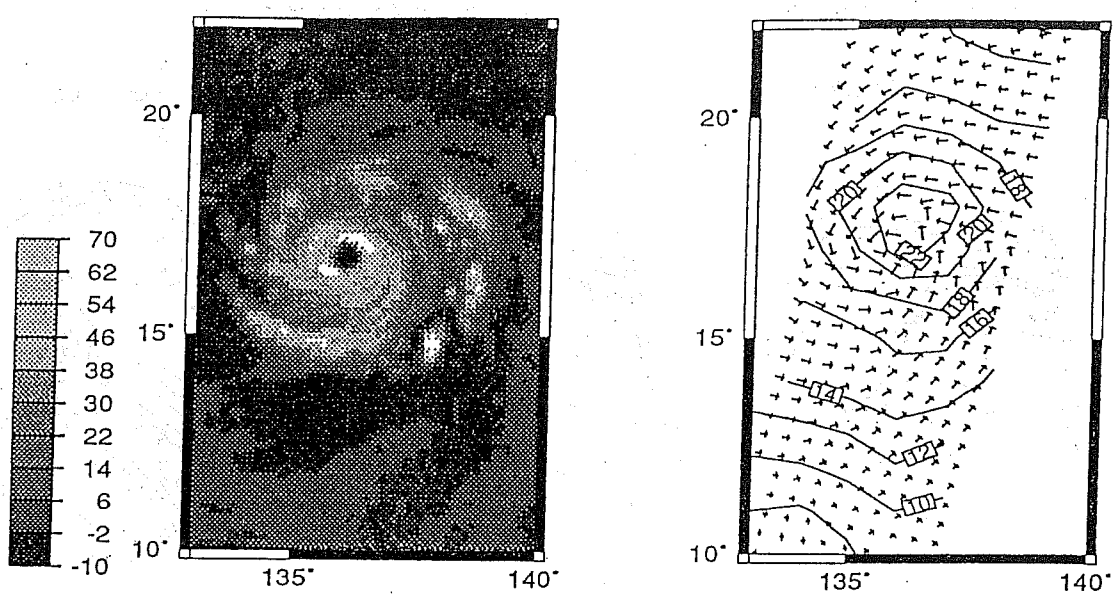

Fig. 6 SSMI scattering index(left) and scatterometer surface winds in Tropical Cyclone ELSIE (92/11/5). Isolines of estimated wind speed are plotted in m/s.(After Quilfen et al, 1994)

(1994) are assimilating SSM/I retrieved water vapor over the sea into a global atmospheric general circulation model (AGCM) with positive effect on cloud water and precipitation produced by the model.

Phoebus and Goerss (1992) have found positive impact of operational assimilation of SSM/I data into the U.S. Navy's Global Atmospheric Prediction System. The U.S. Navy, being part of the defense department, has real time access to SSM/I data.

The integrated cloud liquid water (ICLW) has only recently been a parameter predicted in a realistic manner by numerical models. Raustein *et al.* (1991) compared model estimates based on the Sundqvist *et al.* (1989) model with ICLW obtained from methods based on AVHRR observations in the visible and infrared with estimates based on the 37 GHz liquid water algorithms of Petty (1990) (Figure 7).

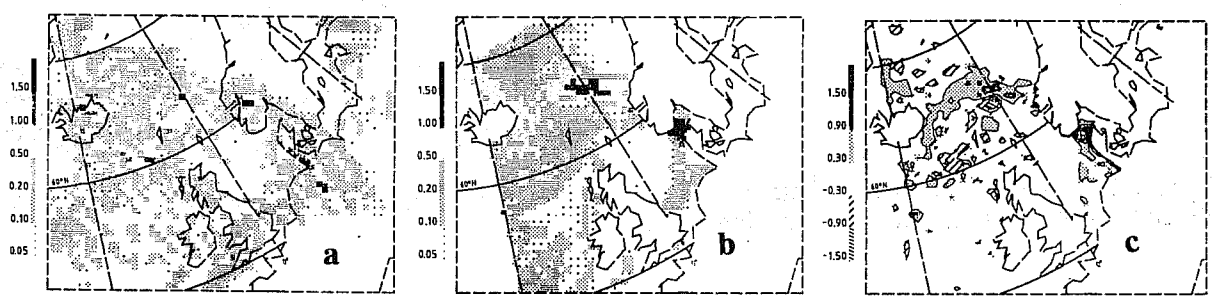

Fig. 7 (a) cloud water content from 30 h of numerical model prediction, valid time 18.00 GMT 27 August 1988, and (b) liquid water amount from interpretation of SSM/I data from the period 17.50 GMT (eastern part) 27 August 1988 to 19.30 GMT (western part) 27 August 1988. (c) The difference field, interpreted water amount (b) minus simulated cloud water content (a). The scale to the left shows the shading for the different amount intervals; unit, kg • m^{-2} (after Raustein et al 1991).

Evaporation rates (latent heat flux)

Liu (1989; 1993) used the bulk aerodynamic method to estimate evaporation rate in the tropics. The input data was SSM/I wind and water vapor content with AVHRR estimates of sea surface temperature. The water vapor gradient is estimated using saturation at the sea surface temperature and a value for the near surface humidity deduced from the IWV given by SSM/I. They found that for the tropics near surface humidity and IWV are highly correlated. Miller and Katsaros (1992) used a modification of the bulk estimation method of Liu (1989) to estimate evaporation rate in the environment of a midlatitude rapidly deepening cyclone. Figure 8 shows the similarity with estimates for a numerical simulation reported by Neiman *et al.* (1990).

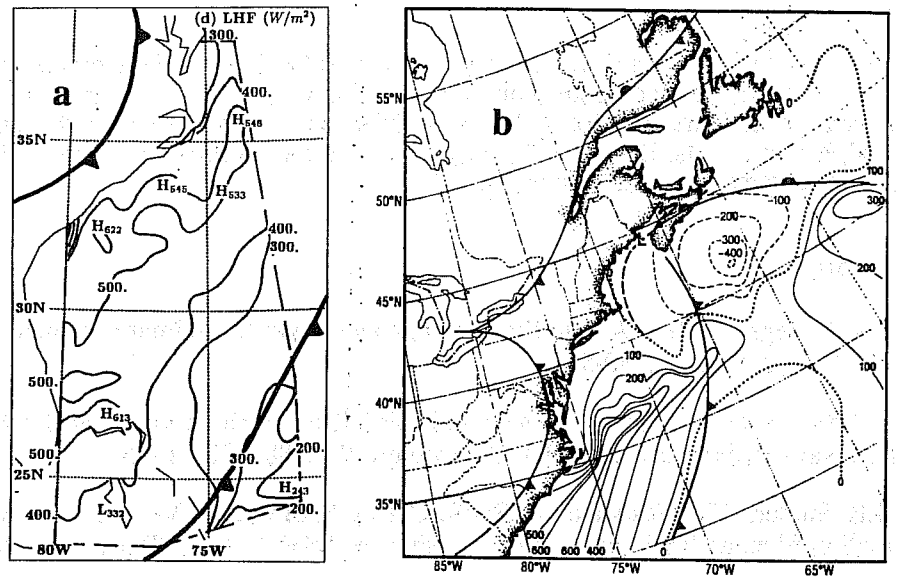

Fig. 8 Surface latent heat flux estimates(Wm^{-2})
a) from SSM/I overpass at 11.00 UTC 26 January 1988 (after Miller and Katsaros 1992).
b) from model calculations at 12.00 UTC 26 January 1988 (after Neiman et al 1990).

Climatological studies

The global perspective of satellites is particularly useful for climate studies and numerous studies of climatic patterns derived from microwave data have appeared, e.g., for SST, Gloersen *et al.* (1992), for water vapor and cloud liquid water, Prabkahara *et al.* (1982; 1983), and for winds. For precipitation the problem of footprint filling makes quantitative estimates difficult (see also review by Petty, 1994).

Liu *et al.* (1994) have carried out a very interesting interpretative study computing climatological flux parameters to attempt to explain the cause and effect of the variations of sea surface temperature, solar radiation, surface winds, and evaporation rate and their relationship to the cloudiness in tropical, deep convection. The evaporation-rate is calculated with the bulk aerodynamic formula (as described in several papers by Liu and colleagues, see above) and the deep convection/cloudiness is obtained from the Outgoing Longwave Radiation (OLR) observed with infrared sensors in the Earth Radiation Budget Experiment (ERBE). They find that proposed simplistic relationships between maximum solar radiation, maximum SST and evaporation, do not hold. There are significant lags in space as well as in time.

Sea ice

Passive microwave observations of the Arctic and Antarctic sea ice covered regions have become operational. The ice concentration and the type of ice, i.e., whether first year or multi-year ice can be determined. Several algorithms have been developed employing polarization differences or variations with frequency (the gradient ratio). The 9-year record of the Nimbus 7 SMMR has been gathered in a volume by Gloersen *et al.* (1992). Season and annual variability, changes in ice extent and in the percentage of open water (in the Arctic) are determined. Such data have tremendous potential for monitoring climate change. The record continues with analysis in a similar manner of SSM/I data. Recently scatterometer measurements by the ERS-1 satellite add similar (and complementary) information (Cavanie *et al.*, 1994). The scatterometer signals are used to delineate the ice edge, which is a practically very important aspect for using the scatterometer winds over the global oceans, since the presence of sea ice drastically contaminates wind estimates and derived quantities such as, for instance, turbulent flux estimates of carbon dioxide or water vapor. A two-frequency narrow beam microwave radiometer is part of the Along Track Scanning Radiometer system on ERS-1 and can also be used for sea ice determinations (Ezraty *et al.*, 1994).

4. CONCLUSIONS

The Special Sensor Microwave/Imager and active microwave systems, scatterometers and altimeters have now reached a state of maturity that operational and research use of these data is extending our forecasting ability and our understanding of the structure of oceanic weather systems. Full understanding of microwave remote sensing of the sea surface and the atmosphere over the ocean requires further development, but it is clear that with more frequent sampling these types of systems will become very valuable.

5. ACKNOWLEDGMENTS

This review has been sponsored by funds from NASA grant NAGW-2633 to the University of Washington, and by the Institut Francais de Recherche pour l'Exploitation de la Mer. I am grateful for the able production of the camera-ready manuscript by Ms. Janet Meadows and assistance with figures by Ms. Kay Dewar and Mr. Ralph Monis. Ms. Hongwei Zhao assisted with the production of Figure 5, and the author thanks Ms. Miletta for comments on the manuscript.

6. REFERENCES

Adler, R.F. and A.J. Negri, 1988: A satellite infrared technique to estimate tropical convective and stratiform rainfall. *J. Appl. Met.*, 27, 30-51.

Alishouse, J.C., 1983: Total precipitable water and rainfall determinations from the Seasat Scanning Multichannel Microwave Radiometer (SMMR). *J. Geophys. Res.*, 88, 1929-1935.

Alishouse, J.C., J.B. Snider, E.R. Westwater, C. Swift, C. Ruf, S. Snyder, J. Vongsathorn, and R.R. Ferraro, 1990a: Determination of cloud liquid water content using the SSM/I. *IEEE Trans. Geosci. Remote Sens.*, 28, 817-822.

Alishouse, J.C., S. Snyder, J. Vongsathorn, and R.R. Ferraro, 1990b: Determination of oceanic total precipitable water from the SSM/I. *IEEE Trans. Geosci. Remote Sens.*, 28, 811-816.

Arkin, P.A. and B.N. Meisner, 1987: The relationship between large-scale convective rainfall and cold clouds over the Western Hemisphere during 1982-1984. *Mon. Wea. Rev.*, 115, 51-74.

Cavanié, A., F. Gohin, Y. Quilfen, and P. Lecomte, 1994: Identification of sea-ice zones using the ami-wind: physical bases and applications to the FDP and Cersat processing chains. In *Proceedings of Second Symposium on ERS-1 in the Service of our Environment,* October 11-14, 1993, Hamburg, Germany, (in press).

Claud, C., K.B. Katsaros, G.W. Petty, A. Chedin, and N.A. Scott, 1992: A cold air outbreak over the Norwegian Sea observed with the Tiros-N Operational Vertical Sounder (TOVS) and the Special Sensor Microwave/Imager (SSM/I). *Tellus*, 44A, 100-118.

Clough, S.A., F.X. Kneizys, G.P. Anderson, E.P. Shettle, J.H. Chetwynd, L.W. Abreu, L.A. Hall, and R.D. Worsham, 1989: FASCOD3: Spectral Simulation. In *IRS'88: Current Problems in Atmospheric Radiation,* J. Lenoble and J.F. Geleyn, eds. A. Deepak Publishing, 372-375.

Curry, J.A., C.D. Ardeel, and L. Tian, 1990: Liquid water content and precipitation characteristics of stratiform clouds as inferred from satellite microwave measurements. *J. Geophys. Res.*, 95, 16,659-16,671.

Ezraty, R., R. Huang, and J. Liu, 1994: Sea-ice detection in the Bohai sea using the ATSR/M and a AVHRR. In *Proceedings of Second Symposium on ERS-1 in the Service of our Environment,* October 11-14, 1993, Hamburg, Germany, (in press).

Glass, M. and G.W. Felde, 1992: Intensity Estimation of Tropical Cyclones Using SSM/I Brightness Temperatures. Preprints, *Sixth Conference on Satellite Meteorology and Oceanography, AMS,* Atlanta, GA., J8-J10.

Gloersen, P.D., D.J. Cavalieri, A.T.C. Chang, T.T. Wilheit, W.J. Campbell, O.M. Johannessen, K.B. Katsaros, K.F. Kunzi, D.B. Ross, D. Staelin, E.P.L. Windsor, F.T. Barath, P. Gudmandsen, E. Langham, and R.O. Ramseier, 1984: A Summary of Results from the First Nimbus-7 SMMR Observations. *J. Geophys. Res.*, 89, 5335-5344.

Gloersen, P., W.J. Campbell, D.J. Cavalieri, J.C. Comiso, C.L. Parkinson, and H.J. Zwally, 1992: Arctic and Antarctic Sea Ice, 1978-1987: Satellite Passive Microwave Observations and Analysis. *Science and Technical Information Program,* National Aeronautics and Space Administration, Washington, D.C., pp. 290.

Goodberlet, M.A., C.T. Swift, and J.C. Wilkerson, 1989: Remote sensing of ocean surface winds with the Special Sensor Microwave/Imager. *J. Geophys. Res.*, 94, 14,547-14,555.

Griffith, C.G., W.L. Woodley, and P.G. Grube, 1978: Rain estimation from geosynchronous satellite imagery -- visible and infrared studies. *Mon. Wea. Rev.*, 106, 1153-1171.

Hollinger, J.P, R. Lo, G. Poe, R. Savage, and J. Pierce, 1987: *Special Sensor Microwave/Imager User's Guide.* Naval Research Laboratory, Washington, D.C., pp. 177.

Katsaros, K.B., 1988: Microwave Remote Sensing of Atmospheric Water Parameters. In *Seminar Proceedings, Data Assimilation Workshop,* 5-9 September 1988, European Centre for Medium Range Weather Forecasts, Reading, England.

Katsaros, K.B., I. Bhatti, L. McMurdie, and G. Petty, 1989: Identification of atmospheric fronts over the ocean with microwave measurements of water vapor and rain. *Weather and Forecasting,* 4, 449-460.

Katsaros, K.B., G.W. Petty, and U. Hammarstrand, 1990: Atmospheric Water Parameters in Mid-Latitude Cyclones Observed by Microwave Radiometry and Compared to Model Calculations. *Technical Report,* Meteorological Institute, University of Stockholm.

Katsaros, K.B. and R.A. Brown, 1991: Legacy of the Seasat Mission for studies of the atmosphere and air-sea-ice interactions. *Bull. Am. Met. Soc.,* 72, 967-981.

Katsaros, K.B., H. Zhao, J. Miletta, and Y. Quilfen, 1993: Monitoring severe storms by passive and active satellite sensors in the microwave frequency range. In *Tropical Cyclone Disasters: Proceedings of ICSU/WMO International Symposium, October 12-16, 1992, Beijing, China,* J. Lighthill, Z. Zhemin, G. Holland, K. Emanuel, eds. Peking Univrsity Press, Beijing, China, 69-78.

Kuo, Y.-H., R.J. Reed, and S. Low-Nam, 1992: Thermal structure and airflow in a model simulation of an occluded marine cyclone. *Mon. Wea. Rev.,* 120, 2280-2297.

Lipes, R.G., R.L. Bernstein, V.J. Cardone, K.B. Katsaros, E.J. Njoku, D.B. Ross, C.T. Swift, and F.J. Wentz, 1979: Seasat scanning multichannel microwave radiometer: result of the Gulf of Alaska workshop. *Science,* 204, 1415-1417.

Liu, W.T., 1989: Moisture and latent heat flux variabilities in the tropical Pacific derived from satellite data. *J. Geophys. Res.,* 93, 6749-6760.

Liu, W.T., W. Tang, and F.J. Wentz, 1992: Precipitable water and surface humidity over global oceans from Special Sensor Microwave Imager and European Center for Medium Range Weather Forecasts. *J. Geophys. Res.,* 97, 2251-2264.

Liu, W.T., 1993: Evaporation from the Ocean. In *Atlas of Satellite Observations Related to Global Change,* R.J. Gurney, J.L. Foster, C.L. Parkinson, eds. Cambridge University Press, 265-278.

Liu, W.T., A. Zhang, and J.K.B. Bishop, 1994: Evaporation and solar irradiance as regulators of sea surface temperature in annual and interannual changes. *J. Geophys. Res.,* (in press).

McMurdie, L.A. and K.B. Katsaros, 1985: Atmospheric water distribution in a mid-latitude cyclone observed by the Seasat Scanning Multichannel Microwave Radiometer. *Mon. Wea. Rev.,* 113, 584-598.

McMurdie, L.A., G. Levy, and K.B. Katsaros, 1987: On the relationship between scatterometer derived convergences and atmospheric moisture. *Mon. Wea. Rev.,* 115, 1281-1294.

McMurdie, L.A. and K.B. Katsaros, 1991: Satellite derived integrated water vapor distribution in oceanic midlatitude storms: variation with region and season. *Mon. Wea. Rev.,* 119, 589-605.

Miller, D.K. and K.B. Katsaros, 1992: Satellite-derived surface latent heat fluxes in a rapidly intensifying marine cyclone. *Mon. Wea. Rev.,* 120, 1093-1107.

Miletta, J., 1993: Meteorological Applications of Coincident Visible, Infrared, and Microwave Observations from the Defense Meteorological Satellite Program. M. Sci. Thesis, Department of Atmospheric Sciences AK-40, University of Washington, Seattle, WA 98195, June 7, 1993, pp.86. (Available on request from K.B. Katsaros.)

Mognard, N.M. and K.B. Katsaros, 1994a: Statistical comparison of the Special Sensor Microwave/Imager and the Geosat altimeter wind speed measurements over the ocean. *The Atmosphere Ocean System,* (in press).

Mognard, N.M. and K.B. Katsaros, 1994b: Weather patterns over the ocean observed with the Special Sensor Microwave/Imager and the Geosat altimeter. *The Atmosphere Ocean System,* (in press).

Neiman, P.J., M.A. Shapiro, E.G. Donall, and C.W. Kreitzberg, 1990: Diabatic modification of an extratropical marine cyclone warm sector by cold underlying water. *Mon. Wea. Rev.*, 115, 2728-2743.

Njoku, E.G. and L. Swanson, 1983: Global measurements of sea surface temperature, wind speed, and atmospheric water content from satellite microwave radiometry. *Mon. Wea. Rev.*, 111, 1977-1987.

Nordberg., W., J. Conaway, D.B. Ross, and T. Wilheit, 1971: Measurements of microwave emission from a foam-covered wind-driven sea. J. Atmos. Sci., 28, 429-435.

Peteherych, S., W.S. Appleby, P.M. Woiceshyn, J.C. Spagnol, and L. Chu, 1988: Application of Seasat scatterometer wind measurements for operational short-range weather forecasting. *Weather & Forecasting,* 3, 89-103.

Petty, G.W., 1990: On the Response of the Special Sensor Microwave/Imager to the Marine Environment - Implications for Atmospheric Parameter Retrievals. Ph.D. Thesis, October 1990, Dept. of Atmospheric Sciences, University of Washington, Seattle, WA 98195, pp. 291. (Requests for copies, copying or reproduction of dissertation: University Microfilms, 300 North Zeeb Road, Ann Arbor, MI 48106.)

Petty, G.W. and K.B. Katsaros, 1990a: New geophysical algorithms for the Special Sensor Microwave/Imager. Preprint Volume, *Fifth International Conference on Satellite Meteorology and Oceanography,* September 3-7, 1990, London, England.

Petty, G.W. and K.B. Katsaros, 1992a: Nimbus-7 SMMR precipitation observations calibrated against surface radar during TAMEX. *J. Appl. Met.*, 31, 489-505.

Petty, G.W. and K.B. Katsaros, 1992b: The response of the SSM/I to the marine environment. Part I. An analytic model for the atmospheric component of observed brightness temperatures. *J. Atmos. & Oceanic Techn.*, 9, 746-761.

Petty, G.W. and K.B. Katsaros, 1994: The response of the SSM/I to the marine environment. Part II. A parameterization of roughness effects on sea surface emission and reflection. *J. Atmos. & Oceanic Techn.,* (in press).

Petty, G.W. and K.B. Katsaros, 1994a: Physical retrievals of over-ocean rain rate from multichannel microwave imagery. Part I: Theoretical characteristics of normalized polarization and scattering indices. *Met. and Atmos. Physics,* (in press).

Petty, G.W. and K.B. Katsaros, 1994b: Physical retrievals of over-ocean rain rate from multichannel microwave imagery. Part II: Algorithm implementation. *Met. and Atmos. Physics,* (in press).

Phoebus, P.A. and J.S. Goerss, 1992: The assimilation of marine surface data into the Navy Operational Global Atmospheric Prediction System. *Marine Technology Society Journal,* 26, 63-72.

Prabkahara, C., H.D. Chang, and A.T.C. Chang, 1982: Remote sensing of precipitable water over the oceans from Nimbus 7 microwave measurements. *J. Appl. Meteor.*, 21, 59-68.

Prabhakara, C., I. Wang, A.T.C. Chang, and P. Gloersen, 1983: A statistical examination of Nimbus-7 SMMR data and remote sensing of sea surface temperature, liquid water content in the atmosphere and surface wind speed. *Bull. Am. Met. Soc.*, 22, 2023-2037.

Quilfen, Y., K. Katsaros, B. Chapron, and H. Zhao, 1994: Surface wind and precipitation patterns in tropical cyclones observed with the ERS-1 scatterometer and with the Special Sensor Microwave/Imager. Proceedings of *"Second Symposium on ERS-1 in the Service of our Environment".* 11-14 October, 1993, Hamburg, Germany, (in press).

Rabin, R.M., L.A. McMurdie, C.M. Hayden, and G.S. Wade, 1991: Monitoring precipitable water and surface wind over the Gulf of Mexico from Microwave and VAS Satellite Imagery. *Weather and Forecasting*, 6, 227-243.

Raustein, E., H. Sundqvist, and K.B. Katsaros, 1991: Quantitative comparison between simulated cloudiness and clouds objectively derived from satellite data. *Tellus*, 43A, 306-320.

Reed, R.J. G.A. Grell, and Y.-H. Kuo, 1993: The ERICA-IOP5 storm. Part I: Analysis and simulation. *Mon. Wea. Rev.*, 121, 1577-1594.

Robertson, F.R. and C. Cohen, 1994: Global analysis of water vapor, cloud and precipitation derived from a diagnostic assimilation of SSM/I geophysical retrievals, (manuscript).

Sand, Aurelie, 1992: Etude d'un systemme frontal par radiometrie hyper frequence spatiale. Ph.D. Thesis, University of Paris VII, pp. 266.

Spencer, R.W., 1986: A satellite passive 37 GHz scattering-based method for measuring oceanic rain rates. *J. Clim. Appl. Meteor.*, 25, 754-766.

Sundqvist, H., E. Berge, and J.E. Kristjánssón, 1989: Condensation and cloud parameterization studies with a mesoscale numerical weather prediction model. *Mon. Wea. Rev.*, 117, 1641-1657.

Wentz, F.J., 1983: A model function for ocean microwave brightness temperatures. *J. Geophys. Res.*, 88, 1892-1908.

Wilheit, T.T. and A.T.C. Chang, 1980: An algorithm for retrieval of ocean surface and atmospheric parameters from the observations of the Scanning Multichannel Microwave Radiometer (SMMR). *Radio Science*, 15, 525-544.

Young, D.F., P. Minnis, K. Katsaros, A. Dybbroe, and J. Miletta, 1992: Comparison of Techniques for Deriving Water-Cloud Microphysical Properties from Multiple Satellite Data. Preprint volume, *11th Internation Conference on Clouds and Precipitation*, Montreal, Quebec, Canada, August 17-21, 1992.